SLAC-PUB-6186
SLAC/SSRL-0029
May 1993
(SSRL/ACD)

Planar Permanent Magnet Multipoles For Particle Accelerator And Storage Ring Applications

Roman Tatchyn

Stanford Synchrotron Radiation Laboratory
Stanford Linear Accelerator Center
Stanford University, Stanford, CA 94309

Abstract

In prior work a planar permanent magnet (PM) configuration for generating an approximate quadrupole field distribution in the vicinity of its symmetry axis was disclosed. In the present paper extensions of the method are considered for generating sextupole and higher order multipole fields. The field distributions and strengths are contrasted with idealized (azimuthally periodic) multipole field generators and selected applications in the area of single-pass and recirculating particle machines are considered.

Submitted to *IEEE Transactions On Magnetics*

Work supported by the US Department of Energy under contract DE-AC03-76SF00515

1. Introduction

Azimuthally periodic multipole field generators, in particular the quadrupole and sextupole, find a wide range of application as focussing and aberration-correcting elements in accelerator and storage ring design [1,2,3]. Conventional structures are typically configured as current-excited axisymmetric permeable yokes with specially contoured salient pole surfaces (e.g., poles shaped as hyperbolic cylinder sections are shown schematized in Fig. 1).

Although multipole structures composed of permeable material (hereafter referred to as iron) are well understood and offer the advantages of effective field delivery and tunability, there are, nonetheless, instances in which the use of iron can exacerbate the complexity and cost of implementing a desired field configuration. For example, in recent work a 60 m long pure-PM undulator with a superimposed iron-based quadrupole focussing/defocussing (FODO) lattice has been designed for Free-Electron Laser (FEL) applications at SLAC [4] (see Figure 2). Analytical studies have shown [5] that the quadrupole yoke facets need to be kept significantly far away from the PM lattice surrounding the undulator axis in order to prevent undesirable modifications of the on-axis field amplitude. Furthermore, at the minimum full aperture (12 cm), a significantly large power consumption by the quadrupoles is necessary in order to attain the required focussing gradients ($\approx$15 T/m). In view of these complications, a special planar "edge-field" permanent magnet (PM) structure has been proposed as a substitute for the iron quads depicted in Fig. 2.

This structure, a generalized form of which is schematized in the top left side of Fig. 3, can generate focussing gradients in excess of 100 T/m with, e.g., four 0.3cm×2cm×4cm blocks of commercially available PM material. With suitable development, the indicated approach could lead to significantly more effective and economical insertion device designs for synchrotron radiation (SR) and FEL applications [6].

In the present paper, the prospects of extending the planar PM quadrupole design to sextupole and higher order multipole structures are systematically explored. Our approach, a generalization of the cited PM quadrupole study, will be based on analyzing the potential functions associated with the general quadrupole and sextupole configurations of Fig. 3, and extending the results to higher order multipoles. Restricting our analysis to PM materials whose magnetization remains unmodified by externally applied fields [7,8], we can simulate the PM field properties by equivalent charge sheets located on the faces perpendicular to the easy axis [9]. Since it is anticipated that the predominant implementations of PM multipoles will consist of materials for which the assumed restriction is true, this should not seriously impair the practical generality of our results.

As may be inferred from the figures, the primary motivation for this investigation is provided by: 1) the evident simplicity, design flexibility, and utility of employing focussing elements with plane-parallel geometries, a wide range of selectable sizes, and fully-open gaps; and 2) the prospect of fabricating such structures both simply and economically.

2. The planar PM quadrupole

Assuming the quadrupole to be centered on z=0 and its length to be sufficiently great for the approximation $L\to\infty$ to be employed, a close approximation to the potential ϕ_Q in the (x,y) plane is easily derived:

$$\phi_Q(x,y) \approx \frac{-B_r}{2\pi}\left\{\left[\left[(X-x)\ln\left(\frac{(X-x)^2+(g'-y)^2}{(X-x)^2+(g'+y)^2}\right) + 2(g'-y)\tan^{-1}\left(\frac{X-x}{g'-y}\right)\right.\right.\right.$$

$$\left.\left.\left. - 2(g'+y)\tan^{-1}\left(\frac{X-x}{g'+y}\right)\right]_{X=-w-\left(\frac{s}{2}\right)}^{X=-\left(\frac{s}{2}\right)} - \left[(X-x)\ln\left(\frac{(X-x)^2+(g'-y)^2}{(X-x)^2+(g'+y)^2}\right)\right.\right.\right.$$

$$\left.\left.\left. + 2(g'-y)\tan^{-1}\left(\frac{X-x}{g'-y}\right) - 2(g'+y)\tan^{-1}\left(\frac{X-x}{g'+y}\right)\right]_{X=\left(\frac{s}{2}\right)}^{X=w+\left(\frac{s}{2}\right)}\right]_{g'-h+\left(\frac{g}{2}\right)}^{g'=\left(\frac{g}{2}\right)}\right\}; \quad (1)$$

To investigate the behavior of this potential in the vicinity of the axis, we perform a Taylor expansion about (x=0,y=0). The general form, including all the dominant terms of interest for investigating the quadrupole and sextupole structures, can be expressed as

$$\phi_i(x,y) \approx \left\{\phi_i(0,0)\right\}^A + \left\{x\left(\frac{\partial\phi_i(0,0)}{\partial x}\right) + y\left(\frac{\partial\phi_i(0,0)}{\partial y}\right)\right\}^B +$$

$$\frac{1}{2}\left\{x^2\left(\frac{\partial^2\phi_i(0,0)}{\partial x^2}\right) + 2xy\left(\frac{\partial^2\phi_i(0,0)}{\partial x\partial y}\right) + y^2\left(\frac{\partial^2\phi_i(0,0)}{\partial y^2}\right)\right\}^C +$$

$$\frac{1}{6}\left\{x^3\left(\frac{\partial^3\phi_i(0,0)}{\partial x^3}\right)+3x^2y\left(\frac{\partial^3\phi_i(0,0)}{\partial x^2\partial y}\right)+3xy^2\left(\frac{\partial^3\phi_i(0,0)}{\partial x\partial y^2}\right)+y^3\left(\frac{\partial^3\phi_i(0,0)}{\partial y^3}\right)\right\}^D +$$

$$\frac{1}{24}\left\{x^4\left(\frac{\partial^4\phi_i(0,0)}{\partial x^4}\right)+4x^3y\left(\frac{\partial^4\phi_i(0,0)}{\partial x^3\partial y}\right)+6x^2y^2\left(\frac{\partial^4\phi_i(0,0)}{\partial x^2\partial y^2}\right)+4xy^3\left(\frac{\partial^4\phi_i(0,0)}{\partial x\partial y^3}\right)\right.$$

$$\left.+y^4\left(\frac{\partial^4\phi_i(0,0)}{\partial y^4}\right)\right\}^E + \frac{1}{120}\left\{x^5\left(\frac{\partial^5\phi_i(0,0)}{\partial x^5}\right)+5x^4y\left(\frac{\partial^5\phi_i(0,0)}{\partial x^4\partial y}\right)+\right.$$

$$10x^3y^2\left(\frac{\partial^5\phi_i(0,0)}{\partial x^3\partial y^2}\right)+10x^2y^3\left(\frac{\partial^5\phi_i(0,0)}{\partial x^2\partial y^3}\right)+5xy^4\left(\frac{\partial^5\phi_i(0,0)}{\partial x\partial y^4}\right)+$$

$$\left.y^5\left(\frac{\partial^5\phi_i(0,0)}{\partial y^5}\right)\right\}^F + \ldots\ , \qquad (2)$$

where $i\varepsilon\{Q,S,O,\ldots\}$, and the grouped terms of total order $0,1,2,\ldots$ have been designated by $A,B,C,\ldots$

Taking the quadrupole expansion out to terms of total order 4, we find for the configuration of Fig. 3 that the potential terms with non-zero coefficients are represented by

$$\phi_Q(x,y) \approx C_{11}xy + E_{13}\{xy^3 - x^3y\} + \ldots\ , \qquad (3)$$

with

$$C_{11} = \frac{-B_r}{\pi}\left[\frac{64g'w(s+w)}{(s^2+4sw+4w^2+4g'^2)(s^2+4g'^2)}\right]_{g'=\left(\frac{g}{2}\right)+h}^{g'=\left(\frac{g}{2}\right)}, \qquad (4)$$

and

$$E_{13} = \frac{B_r}{3\pi}\left[512wg'\left(s+w\right)\left(3s^6+18s^5w+12s^4g'^2+42s^4w^2+48s^3w^3+48s^3wg'^2+\right.\right.$$
$$16s^2w^2g'^2+24s^2w^4-48s^2g'^4-64sw^3g'^2-96swg'^4-192g'^6-96w^2g'^4-$$
$$\left.\left.32w^4g'^2\right)\left(s^2+4g'^2\right)^{-3}\left(s^2+4sw+4w^2+4g'^2\right)^{-3}\right]_{g'=\left(\frac{g}{2}\right)}^{g'=\left(\frac{g}{2}\right)+h}. \qquad (5)$$

In formulating eq. (3), the subscripts on the capital coefficients have been arranged to correspond to the terms with the same (ordered) powers of x and y. Clearly, $E_{31}=-E_{13}$.

It is of interest to examine the dependence of the on-axis field gradients $\partial B_x/\partial y$ and $\partial B_y/\partial x$ on the lateral dimensions of the constituent magnet pieces. In the vicinity of the axis ($|x|, |y| \ll g/2$), s=0, and for w sufficiently large, both gradients can be approximated from the above formulas by (cf. Reference [6])

$$\frac{\partial B_x(x,y,0)}{\partial y} = \frac{\partial B_y(x,y,0)}{\partial x} \approx$$
$$\frac{-8B_r}{\pi g}\left(\frac{\left(\frac{h}{\frac{1}{2}g}\right)}{1+\left(\frac{h}{\frac{1}{2}g}\right)}\right)\left\{1-3\left[\left(\frac{x}{\frac{1}{2}g}\right)^2-\left(\frac{y}{\frac{1}{2}g}\right)^2\right]\left(\frac{1+\left(\frac{h}{\frac{1}{2}g}\right)+\frac{1}{3}\left(\frac{h}{\frac{1}{2}g}\right)^2}{\left\{1+\left(\frac{h}{\frac{1}{2}g}\right)\right\}^2}\right)+\ldots\right\}. \qquad (6)$$

As is intuitively clear, the B_x component increases in the y direction (viz., toward the PM material) and decreases in the x direction, while the B_y component varies in the opposite fashion.

We note that the off-axis x vs. y variations in both gradients are quadratic and symmetric (in terms of gradient strength) about their on-axis values. We can mention here that in the cited prior work [6], it has been shown that rearranging the four PM pieces from the planar quad of Fig. 3 into an orthogonally symmetrized rectangular structure reduces the on-axis field gradients to about 50% of those attainable by the planar configuration.

For s=0 and w≪g, both gradients can be approximated in the vicinity of the axis by

$$\frac{\partial B_x(x,y,0)}{\partial y} = \frac{\partial B_y(x,y,0)}{\partial x} \approx$$

$$\frac{-8B_r}{\pi g}\left(\frac{\left(\frac{h}{\frac{1}{2}g}\right)}{1+\left(\frac{h}{\frac{1}{2}g}\right)}\right)\left(\frac{3\left(\frac{w}{\frac{1}{2}g}\right)^2}{\left\{1+\left(\frac{h}{\frac{1}{2}g}\right)\right\}^2}\right)\left\{\left(1 + 2\left(\frac{h}{\frac{1}{2}g}\right) + \frac{1}{3}\left(\frac{h}{\frac{1}{2}g}\right)^2\right) -\right.$$

$$\left. 10\left[\left(\frac{x}{\frac{1}{2}g}\right)^2 - \left(\frac{y}{\frac{1}{2}g}\right)^2\right]\left(\frac{1 + 2\left(\frac{h}{\frac{1}{2}g}\right) + 2\left(\frac{h}{\frac{1}{2}g}\right)^2 + \left(\frac{h}{\frac{1}{2}g}\right)^3 + \frac{1}{5}\left(\frac{h}{\frac{1}{2}g}\right)^4}{\left\{1 + \left(\frac{h}{\frac{1}{2}g}\right)\right\}^2}\right) + \ldots\right\}. \qquad (7)$$

For a given w and h≪g, we note that gradient strengths in the cited limit will vary more rapidly with the gap than the gradients of eq. (6) by the inverse square of the gap size. The off-axis deviation of the gradients from those of an ideal quadrupole (quad) is evidently also significantly more rapid for w≪g. From simple analytical arguments, we can infer that by continuous variation of the PM quad dimensions (including s) we should be able to design gradient structures that can vary with the inverse square to the inverse fourth power of the gapsize in

a continuously selectable fashion.

3. The planar PM sextupole

As shown in Fig. 3, the planar sextupole structure to be analyzed explicitly allows for a number of degrees of freedom in its implementation. Specifically, the remanent magnetization of the two central pieces can differ by a factor P from that of the four side pieces, there can be a space of (a1-b) between the center and each pair of side pieces, and the side piece thickness h1 can differ from the center piece thickness h. Under the same analytic assumptions as utilized in the preceeding investigation of the PM quadrupole, an analogous expression for the sextupole potential incorporating all the indicated dimensional and magnetic degrees of freedom is straightforwardly derived:

$$\phi_S(x,y) = \frac{-B_r}{2\pi}\left\{\left[\left[(X-x)\ln\left(\frac{(X-x)^2+(g'-y)^2}{(X-x)^2+(g'+y)^2}\right) + 2(g'-y)\tan^{-1}\left(\frac{X-x}{g'-y}\right)\right.\right.\right.$$

$$\left.\left.\left. - 2(g'+y)\tan^{-1}\left(\frac{X-x}{g'+y}\right)\right]_{X=-a1}^{X=-a} + \left[(X-x)\ln\left(\frac{(X-x)^2+(g'-y)^2}{(X-x)^2+(g'+y)^2}\right)\right.\right.\right.$$

$$\left.\left.\left. + 2(g'-y)\tan^{-1}\left(\frac{X-x}{g'-y}\right) - 2(g'+y)\tan^{-1}\left(\frac{X-x}{g'+y}\right)\right]_{X=a1}^{X=a}\right]_{g'=h1+\left(\frac{g}{2}\right)}^{g'=\left(\frac{g}{2}\right)}$$

$$-P\left\{\left[(X-x)\ln\frac{(X-x)^2+(g'-y)^2}{(X-x)^2+(g'+y)^2}+2(g'-y)\tan^{-1}\left(\frac{X-x}{g'-y}\right)\right.\right.$$

$$\left.\left.+2(g'-y)\tan^{-1}\left(\frac{X-x}{g'-y}\right)-2(g'+y)\tan^{-1}\left(\frac{X-x}{g'+y}\right)\right]_{X=-b}^{X=b}\right]_{g'-h+\left(\frac{g}{2}\right)}^{g'-\left(\frac{g}{2}\right)}\Bigg\}; \quad (8)$$

Expanding this potential in compliance with eq. (2), out to terms of total order 5, we find for the general configuration of Fig. 3 that the retained coefficients are associated with the terms of the following expression:

$$\phi_S(x,y) \approx B_{01}y + D_{21}\{3x^2y-y^3\} + F_{41}\{5x^4y-10x^2y^3+y^5\} + \ldots . \quad (9)$$

Evidently, the expansion retains terms of dipole, sextupole, and decapole order, with $D_{21}=-D_{03}$ and $F_{41}=-F_{23}=F_{05}$.

To derive highly simplified expressions for the above coefficients which, nonetheless, can represent configurations of practical interest, we set h=h1 and a1=b. Then,

$$B_{01} = \frac{-4B_r}{\pi}\left[(1+P)\tan^{-1}\left(\frac{b}{g'}\right)-\tan^{-1}\left(\frac{a}{g'}\right)\right]_{g'-\left(\frac{g}{2}\right)+h}^{g'-\left(\frac{g}{2}\right)} \quad (10)$$

$$D_{21} = \frac{4B_r}{3\pi}\left[\frac{g'b(1+P)}{(a^2+g'^2)^2}-\frac{ag'}{(b^2+g'^2)^2}\right]_{g'-\left(\frac{g}{2}\right)+h}^{g'-\left(\frac{g}{2}\right)} \quad (11)$$

and

$$F_{41} = \frac{4B_r}{5\pi}\left[\frac{g'b(1+P)(b^2-g'^2)}{(a^2+g'^2)^4} - \frac{ag'(a^2-g'^2)}{(b^2+g'^2)^4}\right]_{g'=\left(\frac{g}{2}\right)+h}^{g'=\left(\frac{g}{2}\right)} \qquad (12)$$

It is evident that the primary requirement for reducing the potential of eq. (9) to an approximate sextupole distribution is the cancellation of the dipole term coefficient B_{01}. For a given gap g and PM thickness h(-h1), setting eq. (10) equal to 0 will yield all the pairs (a,b) that eliminate the dipole component. Due to the practical utility of using pieces each with the same remanent field, we herewith derive the desired relation between a and b for P=1:

$$\left(\frac{a}{\frac{1}{2}g}\right)^2 - \left(\frac{a}{\frac{1}{2}g}\right)\left\{\frac{\left[1+\left(\frac{h}{\frac{1}{2}g}\right)+\left(\frac{b}{\frac{1}{2}g}\right)^2\right]^2 - \left(\frac{h}{\frac{1}{2}g}\right)^2\left(\frac{b}{\frac{1}{2}g}\right)^2}{2\left(\frac{b}{\frac{1}{2}g}\right)\left[1+\left(\frac{h}{\frac{1}{2}g}\right)+\left(\frac{b}{\frac{1}{2}g}\right)^2\right]}\right\} + \left[1+\left(\frac{h}{\frac{1}{2}g}\right)\right] = 0. \qquad (13)$$

A graph of (a/½g) vs (b/½g) curves derived for (h/½g) values of 0.5, 1, and 2 from the above equation is shown in Fig. 4. As may be deduced from the coefficients of eq. (13), the dimensions b and a cannot exceed limits determined by the choice of (h/½g). Physically, we can interpret this by recognizing that if the dimension 2b/g is too wide, then the outer pieces (which we have constrained to have the same remanent magnetization) will be too far away to cancel the on-axis dipole component generated by the center pieces. Analyzing the roots of eq. (13), we derive the exact constraint on the maximum size of (b/½g), valid in free

space, to be

$$\left(\frac{b}{\frac{1}{2}g}\right) \leq \left(\frac{b}{\frac{1}{2}g}\right)_{MAX} = 1 + \left(1 + \left(\frac{h}{\frac{1}{2}g}\right)\right)^{\frac{1}{2}} + \frac{1}{2}\left(\frac{h}{\frac{1}{2}g}\right) - \frac{1}{2}\left(\frac{12\left(\frac{h}{\frac{1}{2}g}\right)+8+6\left(\frac{h}{\frac{1}{2}g}\right)^2+\left(\frac{h}{\frac{1}{2}g}\right)^3+4\left(1+\left(\frac{h}{\frac{1}{2}g}\right)\right)^{\frac{1}{2}}\left(\frac{h}{\frac{1}{2}g}\right)^2+16\left(1+\left(\frac{h}{\frac{1}{2}g}\right)\right)^{1.5}}{\left(2+\left(\frac{h}{\frac{1}{2}g}\right)\right)}\right)^{\frac{1}{2}}. \quad (14)$$

4. Comparisons with idealized iron quadrupoles and sextupoles

We can now systematically compare selected practical performance characteristics of the PM quadrupole and sextupole with the conventional iron structures of Fig. 1. Of primary interest to our present study are: 1) the maximum near-axis field strength (or gradient) vis-a-vis an iron structure of comparable dimensions, and 2) the radial distance from the z-axis over which the deviation of the PM field from that of an idealized quadrupole or sextupole structure remains sufficiently small. To maximize the attainable PM fields we will take s=0 (quad) and retain a1-b (sextupole).

First, taking the idealized iron quad potential to be given by [3]

$$\phi_Q \approx \frac{B_0}{a'} xy, \quad (15)$$

the effective field-strength (and field-gradient) ratios of the PM vs iron quads can be expressed by η_Q, where

$$\eta_Q = \left|\frac{a'C_{11}}{B_0}\right| \approx \left|\frac{-4B_r a'}{\pi(\frac{1}{2}g)B_0}\right| \left(\frac{\left(\frac{h}{\frac{1}{2}g}\right)}{1+\left(\frac{h}{\frac{1}{2}g}\right)}\right) \left(\frac{3\left(\frac{w}{\frac{1}{2}g}\right)^2}{1+\left(\frac{w}{\frac{1}{2}g}\right)^2}\right) \left\{\frac{1 + \left(\frac{h}{\frac{1}{2}g}\right) + \frac{1}{3}\left(\frac{h}{\frac{1}{2}g}\right)^2 + \frac{1}{3}\left(\frac{w}{\frac{1}{2}g}\right)^2}{1 + 2\left(\frac{h}{\frac{1}{2}g}\right) + \left(\frac{h}{\frac{1}{2}g}\right)^2 + \left(\frac{w}{\frac{1}{2}g}\right)^2}\right\}. \quad (16)$$

Next, we postulate the conditions

$$\left.\begin{array}{l} B_0 = B_r \\ \text{and} \\ a' = \frac{1}{2}g. \end{array}\right\} \quad (I)$$

We justify the first equality by the fact that currently available hard PM materials can attain B_r values of up to approximately 1.3T [10], and at comparable levels of B_0 iron yokes typically start requiring significantly increased levels of excitation to attain marginally higher increments of field strength. Similarly qualitative justification for the second equality may be inferred from Figs. 1 and 3. Issues in contrasting the radial distances (r-a') in Fig. 1 with the PM thicknesses h (and h1) in Fig. 3 are inessential to the following analysis, and will be commented on later.

Under the given assumptions, then, we can tabulate η_Q for selected practical PM thickness/gap (h/g) and width/gap (w/g) ratios, as shown in Table 1. We note that for roughly comparable internal and external dimensions the PM quad can be made about as effective as an iron quad (in the vicinity of its axis), while even for rather thin PM segments, the comparable effectiveness is reduced by only about one half.

To estimate the deviation of the actual PM quad field strength from that of an idealized field distribution, we can express the fractional variations in, respectively, the B_x and B_y components of the two structures (via eq. (3)) as

$$\left[\frac{\Delta B_x}{B_{x(IDEAL)}}\right]_Q \approx \frac{(C_{11}y+E_{13}(y^3-3x^2y))-C_{11}y)}{C_{11}y} = \frac{E_{13}(y^2-3x^2)}{C_{11}}, \quad (17)$$

and

$$\left[\frac{\Delta B_y}{B_{y(IDEAL)}}\right]_Q \approx \frac{(C_{11}x+E_{13}(3xy^2-x^3))-C_{11}x}{C_{11}x} = \frac{E_{13}(3y^2-x^2)}{C_{11}}. \quad (18)$$

Primarily, we are interested in the % deviation of B_x in the y direction for x=0, and of B_y in the x direction for y=0. These can consequently be expressed as, respectively, $C^Q_{wh}(y/g)^2$, and $-C^Q_{wh}(x/g)^2$, with $C^Q_{wh}=100g^2E_{13}/C_{11}$. Calculated values of C^Q_{wh} for selected ranges of practical PM h/g and w/g ratios are shown in Table 2.

Turning to the sextupole, let us now assume that the coefficient B_{01} has been cancelled, and (again to maximize the attainable field strengths) that h1=h and P=1. Then, analogously to the quadrupole, we can, referring to the idealized iron sextupole potential [3]

$$\phi_S \approx \frac{B_0}{3a'^2}(3x^2y-y^3), \quad (19)$$

denote the ratio of the field strength of the PM to the field strength of the iron structure by η_S, where

$$\eta_S = \left|\frac{3a'^2 D_{21}}{B_0}\right| \approx$$

$$\left|\frac{12 B_r a'^2}{3\pi(\tfrac{1}{2}g)^2 B_0}\right| \left\{ \left[\frac{2\left(\frac{b}{\frac{1}{2}g}\right)}{\left\{1+\left(\frac{a}{\frac{1}{2}g}\right)^2\right\}^2} - \frac{\left(\frac{a}{\frac{1}{2}g}\right)}{\left\{1+\left(\frac{b}{\frac{1}{2}g}\right)^2\right\}^2} \right] - \right.$$

$$\left. \frac{1}{\left\{1+\left(\frac{h}{\frac{1}{2}g}\right)^2\right\}^2} \left[\frac{2\left(\frac{b}{h+\frac{1}{2}g}\right)}{\left\{1+\left(\frac{a}{h+\frac{1}{2}g}\right)^2\right\}^2} - \frac{\left(\frac{a}{h+\frac{1}{2}g}\right)}{\left\{1+\left(\frac{b}{h+\frac{1}{2}g}\right)^2\right\}^2} \right] \right\}. \qquad (20)$$

Next, assuming that the postulated conditions (I) for performing the PM/iron quadrupole comparison remain valid for the sextupole, ranges of variation of η_S as functions of the gap-normalized dimensions a/g and b/g can be straightforwardly calculated for selected practical h/g ratios, as is done in Table 3. As in the case of the PM quad, we note that the field-delivery effectiveness of the PM sextupole can be made approximately equal to that of the corresponding azimuthally periodic iron structure for comparable internal and external dimensions. It is, furthermore, remarkable that this effectiveness gets reduced by only about a half for the appreciably small values tabulated for $(h/\tfrac{1}{2}g)$.

To assess the departure of the actual PM sextupole field strength components B_x and B_y from those of the idealized field distribution, we can use eq. (9) to express their fractional

deviations vs. x and y as

$$\left[\frac{\Delta B_x}{B_{x(IDEAL)}}\right]_S \approx \frac{(D_{21}\{6xy\}+F_{41}\{20x^3y-20xy^3\})-D_{21}\{6xy\}}{6D_{21}xy} = \frac{10F_{41}\{x^2-y^2\}}{3D_{21}}, \tag{21}$$

and

$$\left[\frac{\Delta B_y}{B_{y(IDEAL)}}\right]_S \approx \frac{(3D_{21}\{x^2-y^2\}+F_{41}\{5x^4-30x^2y^2+5y^4\})-3D_{21}\{x^2-y^2\}}{3D_{21}\{x^2-y^2\}} = \frac{5F_{41}\{x^4-6x^2y^2+y^4\}}{3D_{21}\{x^2-y^2\}}. \tag{22}$$

We first note that the B_x component vanishes to both sextupole and decapole orders along the x and y axes. Consequently, we can choose some alternative convenient direction represented by, say, $y=\alpha x$, to assess the behavior of B_x. Regarding B_y, we are interested in its deviations from the corresponding ideal sextupole component both along x (for y=0) and y (for x=0). Choosing $\alpha \approx 35.26°$, all three relative deviations can be conveniently expressed as: 1) $C^S_{bh}(x/g)^2$ (for B_x along $y=x/2^{1/2}$); 2) $-C^S_{bh}(y/g)^2$ (for B_y along the y axis; and 3) $C^S_{bh}(x/g)^2$ (for B_y along the x axis); where $C^S_{bh}=500g^2F_{41}/3D_{21}$. Calculated values of C^S_{bh} for selected ranges of practical PM h/g and b/g ratios are given in Table 4. Of particular interest is the change of sign evident in the tabulated values for parameters

corresponding to significantly effective field delivery (i.e., for $0.5 \leq \eta_S \leq 1$). This indicates that practically useful values of (h/½g), (a/½g), and (b/½g) can be sought that will not only zero the coefficient B_{01}, but that can also reduce F_{41} to substantially small values, leading to a nearly ideal sextupole field in the vicinity of the axis. A convenient polynomial equation (for P=1) for helping to numerically identify these values may be expressed as $B_{01}^2+F_{41}^2=0$.

5. Higher order multipoles

Higher order multipoles can be designed either by heuristic extensions of the basic planar quadrupole and sextupole structures, or by the more rigorous application of the analytical method utilized in this paper to each case of interest.

Heuristically, the quadrupole and sextupole configurations of Fig. 3 may be perceived as the basic elements out of which multipoles of progressively higher multiples of four can be constructed. Thus, a repetition of the quadrupole structure can be used to generate octupoles, dodecapoles, hexadecapoles, etc.; while a repetition of the sextupole structure can be used to generate decapoles, tetradecapoles, octodecapoles, etc. As indicated in Fig. 5, the configurational possibilities and degrees of freedom can grow rapidly for planar structures with constant gaps. A systematic way to assess the alternatives can be based on realizing that the primary function of each additional

structure is to cancel the lowest order multipole field that the already existing structure is generating without cancelling the next higher multipole order. Thus, the outside four pieces in the top left configuration of Fig. 5, having different (specifically, higher) remanent fields than the inside four pieces, can be designed to cancel the quadrupole gradients generated by the inside pieces; but, as may be verified from direct parameter substitution, the coefficients E_{13} for each set of pieces will not in general cancel, leaving a first-order octupole potential in the vicinity of the axis. The same type of quadrupole cancellation can obviously be made to occur with the planar configuration in the lower left hand side of Fig. 5. To cancel the octupole components, an additional structure consisting of 2 superimposed quadrupoles (eight additional pieces) would evidently have to be added to the depicted structures. The general resulting rule is that with this approach at most 2×2^N pieces would be required to synthesize a 4N-pole potential.

As depicted on the right side of Fig. 5, essentially the same method can be utilized with the sextupole. For the top right configuration, the two central pieces associated with the outside four pieces do not have to be physically placed, but can be effected by suitably modifying the magnetization across the faces of the existing central pieces. For the configurational approach on the bottom right, at most 3×2^N pieces would evidently be required to generate successively higher (2+4N)-pole potentials.

Apart from these intuitively systematic approaches to multipole synthesis, it is also analytically evident that it

should be possible to generate higher order multipoles more economically with either 4N pieces for integral multiples of the quadrupole, or with 6N pieces for the "4N+2" extensions of the sextupole. In both cases, it is required that there be enough degrees of freedom in the magnet piece dimensions and remanent fields to simultaneously null the undesired lower multipole component coefficients while retaining the desired one. This approach, while analytically more taxing, represents a more efficient use of material. For N not too large, each approach may be queried with regard to the field quality and amplitude desired for a given application.

6. Tolerances

From the evident dependence of the quadrupole, sextupole, and higher-order PM multipole fields on the dimensional, positional, and field symmetries of the individual permanent magnets that constitute them (as follows from the explicit forms of equs. (1) and (8)), it should be evident that the sensitivity of the attained field profile to the errors associated with these symmetries can become significant, especially for structures in which increasingly large numbers of magnet pieces need to be deployed (e.g., Fig. 5). To assist us in examining this issue quantitatively, we will appeal to the notion of the differential sensitivity of a system parameter x to a system variable y on which it depends. This can be expressed as

$$S_y^x = \frac{y}{x}\left(\frac{\partial x}{\partial y}\right) = \frac{\partial(\ln(x))}{\partial(\ln(y))}, \tag{22}$$

and can be interpreted as the fractional change in x induced by a fractional change in y. If all the (say, M) variables affecting x are designated by an index, viz., y_i, and if each variable is assumed to vary independently with a normal distribution, the net rms fractional variation in x can be expressed as

$$\left[\sum_{i=1}^{M}\left(S_{y_i}^x\right)^2\right]^{1/2}. \tag{23}$$

For equal sensitivities, this expression varies as $M^{1/2}$. For interdependent y_i, the linear sum of the sensitivities can be used to assess the desired fractional change in x.

A comprehensive discussion and analysis of the specific types of errors and tolerances associated with the general multipole structures introduced in the preceding sections is not within the scope of this paper. For both practical and illustrative purposes, however, we will briefly discuss the specific dependence of the net dipole term B_{01} of the sextupole structure in Fig. 3 on a selected set of tolerances of its constituent pieces.

A realistic simplifying assumption that can be made is that the four end magnets of Fig. 3 would ordinarily be prepared from a single machined and magnetized piece, as would the two middle magnets. Under this assumption, any deviations in the the

parameters P, b, and a of eq. (1) can be assumed to be the same for the relevant magnet groups. Under the cited conditions, then, we get:

for a=b,

$$S_P^{B_{01}} = \frac{P}{B_{01}} \frac{\partial B_{01}}{\partial P} = 1 \; ; \qquad (24)$$

for a=b,

$$S_b^{B_{01}} = \frac{b}{B_{01}} \frac{\partial B_{01}}{\partial b} = \frac{\left(b+\frac{b}{P}\right)\left\{\frac{g}{2}\left(b^2+\left(\frac{g}{2}\right)^2\right)^{-1} - \frac{g+2h}{2}\left(b^2+\left(\frac{g+2h}{2}\right)^2\right)^{-1}\right\}}{\tan^{-1}\left(\frac{2b}{g}\right) - \tan^{-1}\left(\frac{2b}{g+2h}\right)} \; ; \qquad (25)$$

and, for P=0,

$$S_a^{B_{01}} = \frac{a}{B_{01}} \frac{\partial B_{01}}{\partial a} = \frac{a\left\{\frac{g}{2}\left(a^2+\left(\frac{g}{2}\right)^2\right)^{-1} - \frac{g+2h}{2}\left(a^2+\left(\frac{g+2h}{2}\right)^2\right)^{-1}\right\}}{\tan^{-1}\left(\frac{2b}{g}\right)-\tan^{-1}\left(\frac{2b}{g+2h}\right)-\tan^{-1}\left(\frac{2a}{g}\right)+\tan^{-1}\left(\frac{2a}{g+2h}\right)} . \qquad (26)$$

Choosing P=1, B_r=1T, a=0.5282cm, b=0.175cm, g=1cm, and h=0.5cm (cf. Table 3), the sensitivities of equs. (25) and (26) become 1.74 and -0.22, respectively. Thus, for example, for a 0.7% tolerance in b (±0.025mm), the corresponding tolerance on the dipole field component appearing on the axis would be ± 25gauss.

Regarding the general impact of tolerances on the field quality of planar PM multipoles, it is important to note that not only does the minimal number of independent variables vary

relatively proportionately to the minimal number of magnet pieces (viz., 4N for quads and 6N for sextupoles), but that the number of system parameters contributing to the various possible field abberations can also grow proportionately to N (for N not too large). This can be ascertained directly from assessing the number of individual terms of the Taylor expansion of a general multipole potential as extrapolated from eq. (2). Specifically, if any of the tolerances of the constituent magnet pieces induce the appropriate asymmetries in the field potential, many of the displayed differential coefficients will display non-zero values. Thus, the overall number of contributions to field imperfections will grow proportionately with N^2.

To estimate their net effect on a multipole field, we can make the following worst-case assumptions: 1) most of the system dimensional and magnetization parameters are independent; 2) each of the multipole magnet pieces displays errors in a significant number of such parameters (nominally, the 2 lateral PM block dimensions, the 5 relevant variables of position and inclination, and the 4 variables associated with field strength and direction); and 3) the corresponding sensitivity of B_{01} to each of these is of the order of 1. Then, quadratically compounding the sensitivity of a <u>single</u> field parameter to the M configuration variables (see expression (23) above) with the number of such parameters (proportional to N) yields the result that the overall rms sensitivity of the field quality to the magnet tolerances will be proportional to fN, where f is some number significantly larger than 1. From the above calculated

example, this result clearly indicates that tolerance issues will rapidly start becoming problematical for conventionally-machined planar PM structures that feature small dimensions and that are significantly more complicated than the quadrupole or sextupole.

7. Discussion

We have described a systematic method for designing and configuring planar PM multipoles, in particular the quadrupole and sextupole. To assess the expected performance of the latter structures, we have systematically compared their attainable field strength to iron structures of similar dimensions. This comparison, based on a heuristic set of simplifying assumptions, was nominal, and should be used as only one factor when assessing the specific advantages or disadvantages of the PM vs. iron structures for any given application of interest. For example, when gaps at the level of 1 cm or less are involved, the PM multipole can be expected to attain higher fields with smaller outside dimensions than the iron devices of Fig. 1, since the outside diameter r of the latter structures would need to be made large enough to accomodate the ampere-turns necessary for generating comparable fields. Alternatively, the iron devices may display both economical and field quality advantages at larger scales of size due to the larger quantities of PM material that would be required to fabricate multipole structures of comparable field quality and homogeneity. Nevertheless, it is noteworthy

that insofar as the practical attainment of maximum field gradients vs. aperture size is concerned, both the iron vs. planar PM quad and iron vs. planar PM sextupole appear to be about equally effective.

To establish the extent of the region about the planar PM axis over which usable (i.e., substantially pure) quadrupole and sextupole fields exist, we have also systematically analyzed the deviation of the actual PM quadrupole and PM sextupole fields from the corresponding idealized fields vs. distance from the axis. For operation at either small or large gaps, the essential result is that it should be, in principle, possible to design either quadrupoles or sextupoles for which this deviation is limited to only a few percent over an axis-centered diameter of about one fifth the gap size.

A basic question addressed by the present study concerns the possible applications of the planar PM multipoles. Referring to their iron counterparts, perhaps the most obvious potential use is as lattice or stand-alone optical elements on linear and circular particle accelerators [6]. In this respect, the compact profile, open gap, and comparable field-delivery effectiveness of the PM elements imply superior convenience for installation and access, potential advantages for particle-beam research applications. On the other hand, both the asymmetry and limited extent of the vertical vs. horizontal field homogeneity could potentially limit planar PM optics to either linear single-pass machines or to recirculating machines with substantially small dynamic apertures. Another potential drawback is the apparently

limited range of field tunability, which could restrict the use of planar PM optics to machines with limited ranges of operating and injection energies. Regardless of these potential limitations, however, it can be expected that further development and study of the field characteristics of planar PM multipoles (including their asymmetries) should establish selected areas of particle accelerator design and operation for which the dimensional and geometric parameters of such elements are optimally suited.

Other, more specific areas of application suggested by the relatively high gradients, open gaps, and compact sizes of the PM elements could include: 1) the development of 4th generation compact storage ring lattices [11], 2) development of mini-beta sections on conventional linear or circular machines for micropole undulator applications [12], 3) the implementation of focussing and transport lattices for slow neutrons (quadrupoles) [13], 4) the development of specialized focussing lattices composed of quadrupoles or sextupoles, or both, for enhancing the gain of FELs [6], and 5) the development of electric motor structures with planar field-generating configurations (4N or 2+4N poles).

Considerations for tuning the fields of planar PM multipoles can, in general, differ with respect to the multipole order. In a prior note [6], for example, a number of possible methods of tuning a PM quadrupole were noted. These included: 1) varying the vertical gap g and horizontal gap s; 2) superimposing the field from a current-controlled "cos2θ" coil (when small

fieldvariations about a fixed value are desired); and 3) varying the proximity of permeable planes placed symmetrically above and below the quad elements (tuning by images). It was also shown that PM quad elements could be installed between the (suitably symmetric) iron pole faces in an undulator gap without having their first-order focussing properties seriously altered by the induced image fields. Unfortunately, simple considerations indicate that for sextupoles and higher 4N or 2+4N poles, the 1st and 3rd tuning methods (based, in essence, on variation of the single parameter g) will not be, in general, applicable. This follows from the observation that if all the lateral dimensions are fixed, the gap in the higher order PM elements needs to remain constant in order to maintain the cancellation of the undesired lower-order field components. Thus, to employ mechanical tuning that would maintain the desired cancellation, more degrees of freedom, viz., provisions for independent mechanical x-y motion of the individual elements of the multipole would evidently be required. In spite of this, we may note that for certain applications this complication can be minimized or even avoided for the planar PM sextupole. Thus, for example, if a sextupole focussing lattice is installed in a PM undulator gap, and the lattice period is an integral multiple of the undulator period, tuning by images from outside the undulator lattice will activate the B_{01} (dipole) component of the sextupole field, but this will just add in phase with the undulator dipole field, leading to typically inessential changes in the undulator radiation characteristics. Similarly, when planning a focussing

sextupole lattice for the gap of an undulator with iron poles (see Fig. 6), the sextupole design can be "pre-corrected" for the B_{01} contributions from the expected image fields, so that upon installation the net dipole contributions from the actual and image elements will in fact cancel. Clearly, analogous mitigating strategies based on single-parameter (viz., gap) tuning for higher order multipoles will tend to become significantly more difficult to implement under general circumstances. Thus, for all practical purposes, optimal approaches to the simple tuning of planar PM 4N and 2+4N poles with N>1 would appear to imply the utilization of external fields from non-permeable multipole current distributions.

Selected analytical aspects of tolerances in the constituent magnets of the planar PM multipoles were discussed in a prior section. A number of related practical issues deserve attention. From the basic sensitivity relation (eq. (22)) it is evident that multipole size is a primary factor in the attainable field quality. This follows from the fact that attainable machining tolerances are typically fixed, and will thereby constitute a smaller fractional deviation in a magnet's dimensions for a larger work piece. Second, at smaller scales of size the field quality of a magnet will no longer remain fully independent of dimensional and mechanical errors, but will start becoming influenced by them. Thus, the bigger the multipole, the more forgiving the dimensional and positional tolerances. Regarding the inherent field quality of the magnet pieces in general (as measured, say, by its constancy of strength and direction over

the surface of a given magnet), it is well known that the best commercially available materials can exhibit fractional field variations of the order of 10^{-3}. Should this level of field tolerance need to be reduced even further, recent strategies (developed for undulator construction) based on fabricating the chosen magnet out of a population of smaller, precisely characterized and sorted, magnets could be employed [14,15,16]. Another, still largely-unexplored approach would be to investigate the development of alternative magnet fabrication techniques that could incorporate this type of statistical control of field quality at the materials or block preparation stage.

Finally, a number of additional issues meriting further systematic investigation appear to be suggested by the present study. First, the effect of deviations from the assumed physical model of the PM material on the analytical forms derived in this paper should be explored. Although it is anticipated that the appropriate control of such deviations by use of symmetry cancellations (for sufficiently small deviations) should help to maintain the first-order applicability of the present formalism, it should be of value to explicitly verify which additional classes of PM materials could be employed for fabricating high-quality planar PM multipoles. Another useful analytical extension of the present study would be to rederive expressions, or computational algorithms, for planar multipole magnet pieces of finite length. This will evidently be necessary, for example, for: 1) the accurate calculation of the fields of short

structures with large gaps, 2) the synthesis of long multipoles out of shorter ones to attain a non-constant field amplitude variation along the z direction, and 3) the calculation of contributions to the on-axis field from higher-order image fields when the multipole is operated between iron pole surfaces. Finally, a systematic study of the focussing and aberration-correcting properties of planar multipoles in particle-beam optical systems would appear to be of value. In particular, their vertical vs. horizontal asymmetries make them essentially different, in a global sense, from the more thoroughly understood azimuthally symmetric structures of Fig. 1, raising the possibility that these differences could lead to applications of practical interest.

6. Acknowledgements

Useful comments by members of the Linac Coherent Light Source (LCLS) research group are acknowledged. This research was performed at SSRL which is operated by the Department of Energy, Office of Basic Energy Sciences, Division of Chemical Sciences. That Office's Division of Materials Sciences has provided support for this research.

Table 1.

Selected field strength ratios η_Q of planar PM vs. azimuthally periodic iron quadrupoles for selected PM widths w and thicknesses h.*

h/g = 0.25	h/g = 0.5	h/g = 1
$0.05 \leq w/g \leq 1$	$0.05 \leq w/g \leq 1$	$0.05 \leq w/g \leq 1$
$0.009 \leq \eta_Q \leq 0.475$	$0.011 \leq \eta_Q \leq 0.7$	$0.012 \leq \eta_Q \leq 0.89$

* Pole-face field B_0 of the iron quad assumed equal to the PM remanent field B_r. Iron quad aperture radius a' assumed equal to the PM quad half-gap size g/2.

Table 2.

Coefficients C^{Q}_{wh} for calculating the percentage deviation of the planar PM quad field components from those of an ideal quadrupole field distribution in the vicinity of the symmetry axis.

h*/g^ →	0.125	0.25	0.5	1
w**/g ↓	C^{Q}_{wh} ↓	C^{Q}_{wh} ↓	C^{Q}_{wh} ↓	C^{Q}_{wh} ↓
0125	1004	903	812	757
0.25	789	720	650	604
0.5	448	416	380	352
1.0	297	261	225	200
2.-	305	262	215	177

* thickness of all the PM segments

** width of all the PM segments

^ full quadrupole gap size

Table 3.

Selected field strength ratios η_S of planar PM vs. azimuthally periodic iron sextupole structures for selected PM segment widths: a-b (ends) and 2b (center).* All segment thicknesses = h.

h/g = 0.25	h/g = 0.5	h/g = 1
$0.05 \leq b/g \leq 0.16$	$0.05 \leq b/g \leq 0.175$	$0.05 \leq b/g \leq 0.2$
$0.1022 \leq a/g \leq 0.5247$	$0.1018 \leq a/g \leq 0.5282$	$0.1015 \leq a/g \leq 0.6015$
$0.0152 \leq \eta_S \leq 0.55$	$0.0183 \leq \eta_S \leq 0.78$	$0.0184 \leq \eta_S \leq 0.96$

* Pole-face field B_0 of the iron sextupole assumed equal to the PM remanent field B_r. Iron sextupole aperture radius a' assumed equal to the PM sextupole half-gap size g/2.

Table 4.

Coefficients C_{bh}^{S} for calculating the percentage deviation of the planar PM sextupole field components from those of an ideal sextupole field distribution in the vicinity of the symmetry axis.

h*/g^ →	0.125	0.25	0.5	1
b**/g ↓	C_{bh}^{S} ↓	C_{bh}^{S} ↓	C_{bh}^{S} ↓	C_{bh}^{S} ↓
0.04	-631	-581	-546	-534
0.08	-513	-479	-453	-444
0.12	-298	-325	-306	-307
0.16	175	97	-79	-127
0.20	—	—	—	172

* thickness of all the PM segments

** half-width of the center PM segments

^ full sextupole gap size

7. References

[1] M. S. Livingston and J. P. Blewett, Particle Accelerators, McGraw-Hill, New York, 1962.

[2] E. Regenstreif, "Focusing with Quadrupoles, Doublets, and Triplets," in Focusing of Charged Particles, A. Septier, ed., Academic Press, New York, 1967. pp. 353-410.

[3] D. C. Carey, The Optics of Charged Particle Beams, Harwood Academic Publishers, New York, 1987.

[4] C. Pellegrini, J. Rosenzweig, H.-D. Nuhn, P. Pianetta, R. Tatchyn, H. Winick, K. Bane, P. Morton, T. Raubenheimer, J. Seeman, K. Halbach, K.-J. Kim, and J. Kirz, "A 2 to 4 nm High Power FEL on the SLAC Linac," presented at the 1992 FEL Conference, August 1992, Kobe, Japan; to appear in Nucl. Instr. and Meth. 1993.

[5] R. Tatchyn, unpublished.

[6] R. Tatchyn, "Permanent Magnet Edge-Field Quadrupoles as Compact Focussing Elements for Single-Pass Particle Accelerators," SLAC/SSRL ACD-Note No. 010, March 1993.

[7] J. D. Jackson, Classical Electrodynamics, John Wiley&Sons, Inc., 1975, p. 187 et ff.

[8] K. Halbach, "Design of Permanent Multipole Magnets with Oriented Rare Earth Cobalt Materials," Nuclear Instruments and Methods 169, 1(1980).

[9] R. Tatchyn and P. L. Csonka, "Submillimeter Period Undulators: New Horizons in Insertion Device Technology," in Proceedings of the Adriatico Research Conference on Undulator Magnets for Synchrotron Radiation and Free Electron Lasers, R. Bonifacio, L. Fonda, and C. Pellegrini, eds., Trieste, Italy, 23-26 June, 1987, p. 71.

[10] Anil Nanji, Magnet Sales and Manufacturing, Inc., private communication.

[11] M. Cornacchia and H. Winick, eds., Proceedings of the Workshop on Fourth Generation Light Sources, SSRL, February 24-27, 1992, SSRL Publication No. 92/02.

[12] R. Tatchyn, P. Csonka, and R. Tatchyn, "Perspectives on micropole undulators in synchrotron radiation technology," Rev. Sci. Instrum. 60(7), 1796(1989).

[13] As shown in reference [6], planar PM quadrupoles with millimeter-sized apertures could attain gradients in the range of 10^3-10^4 T/m. Taking the neutron magnetic moment to be approximately 10^{-26}J/T, a 1m long quadrupole of this strength could induce deflection angles of the order of 1mr

for 400°K thermal neutrons.

[14] A. D. Cox and B. P. Youngman, "Systematic selection of undulator magnets using the technique of simulated annealing," SPIE Proceedings No. 582, 91(1986).

[15] G. Rakowsky, "Considerations for Optimizing the Performance of Permanent Magnet Undulators," Proceedings of the Workshop on Fourth Generation Light Sources, M. Cornacchia and H. Winick, eds., SSRL, Feb. 24-27, 1992, SSRL Publication No. 92/02, p. 405.

[16] L. Solomon, "Magnet Block Placement Considerations in Hybrid Insertion Devices at the NSLS," ibid., p. 603.

Figure Captions

Figure 1. Schematic midplane front views of an iron-yoke quadrupole (left) and sextupole (right). Coil structures for exciting the salient pole fields are not shown. The indicated pole face contours are hyperbolic segments.

Figure 2. Pure PM undulator design prototype for the Stanford Linear Accelerator Linac Coherent Light Source with a superimposed quadrupole lattice field generated by iron-based quadrupoles.

Figure 3. Schematic midplane front views of the planar permanent magnet edge-field quadrupole (left) and sextupole (right).

Figure 4. Values of $a/\frac{1}{2}g$ vs. selected values of $b/\frac{1}{2}g$ and $h/\frac{1}{2}g$ for nulling the on-axis dipole component of the planar PM sextupole. With reference to Fig. 3, P=1, h=h1, and a1=b are assumed.

Figure 5. Alternative heuristic schemes for extending planar multipole construction beyond the quadrupole and sextupole. The left figures show alternative approaches for implementing octupoles, dodecapoles, etc. The right figures indicate possible approaches for implementing decapoles, tetradecapoles, etc.

Figure 6. Arrangement of an edge-field sextupole lattice in the gap of an insertion device with permeable poles. By centering the PM pieces over the iron pole faces and keeping the same periodicity as the undulator structure (or some multiple of it), virtually identical modulation of both the sextupole fields and the undulator's dipole field by the proximity effects of the iron poles is ensured.

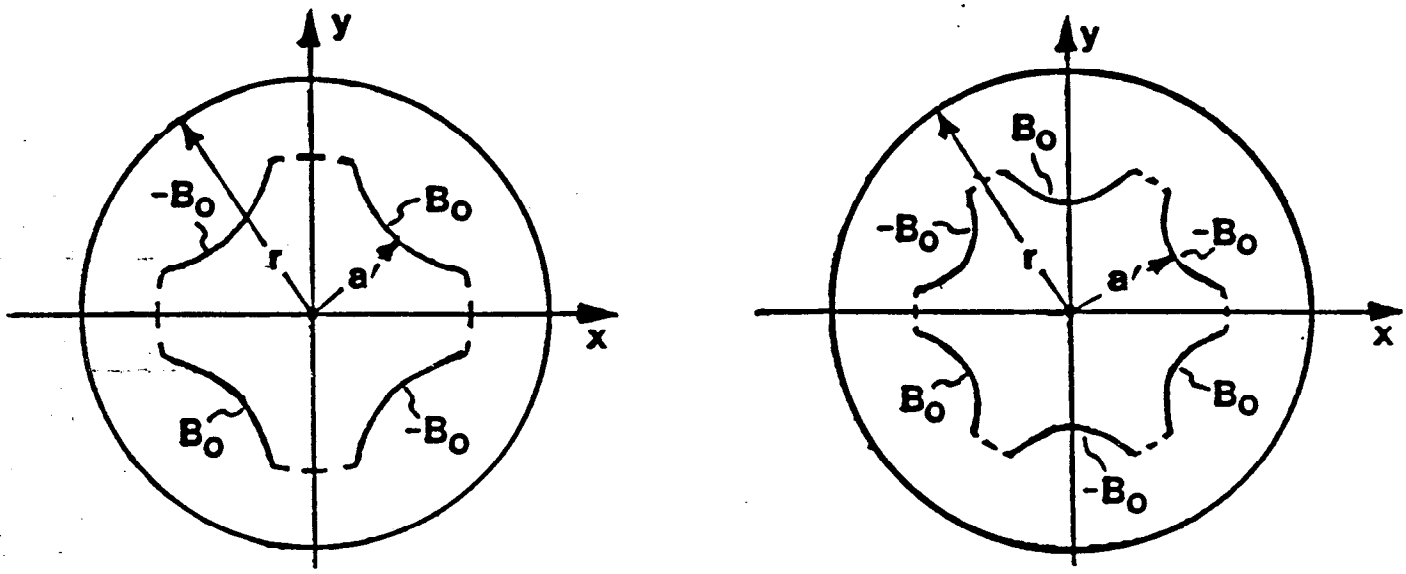

Fig. 1

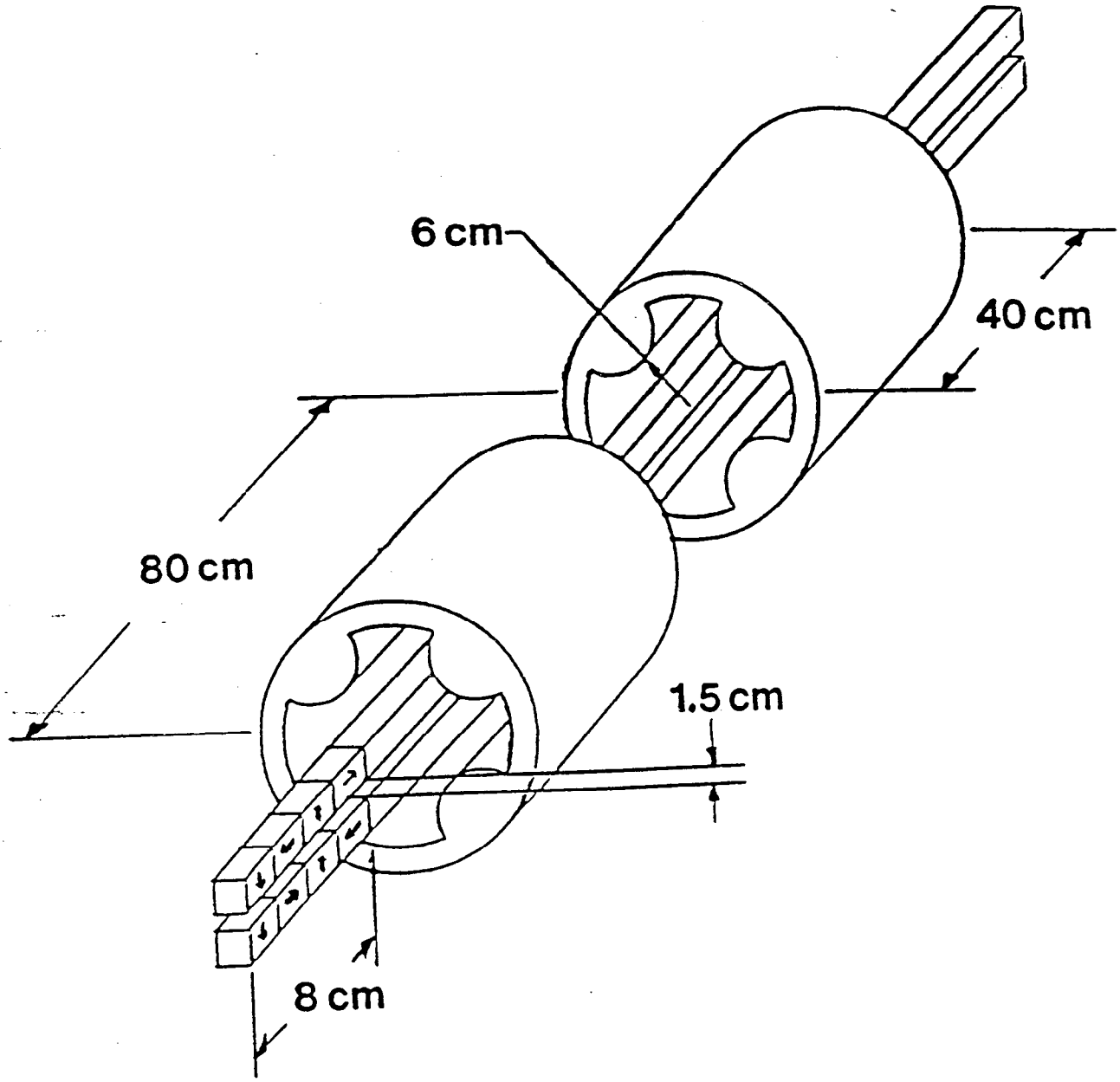

Fig. 2

PLANAR PM QUADRUPOLE

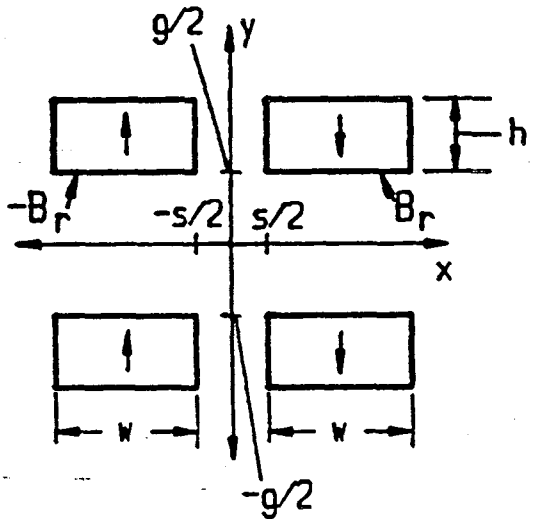

PLANAR PM SEXTUPOLE

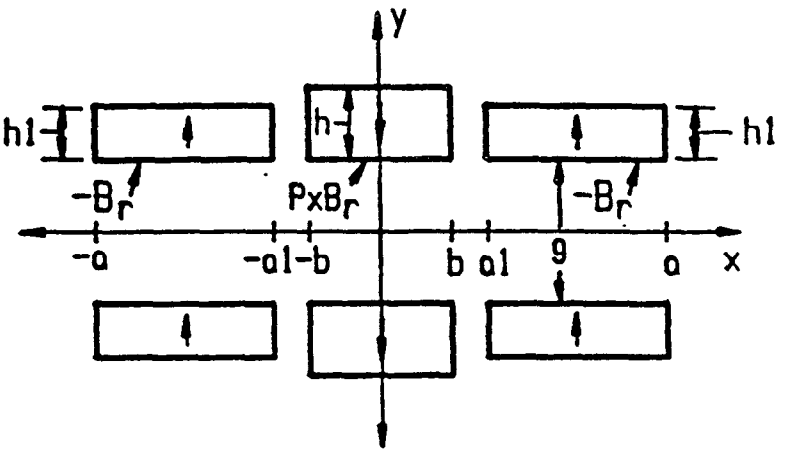

Fig. 3

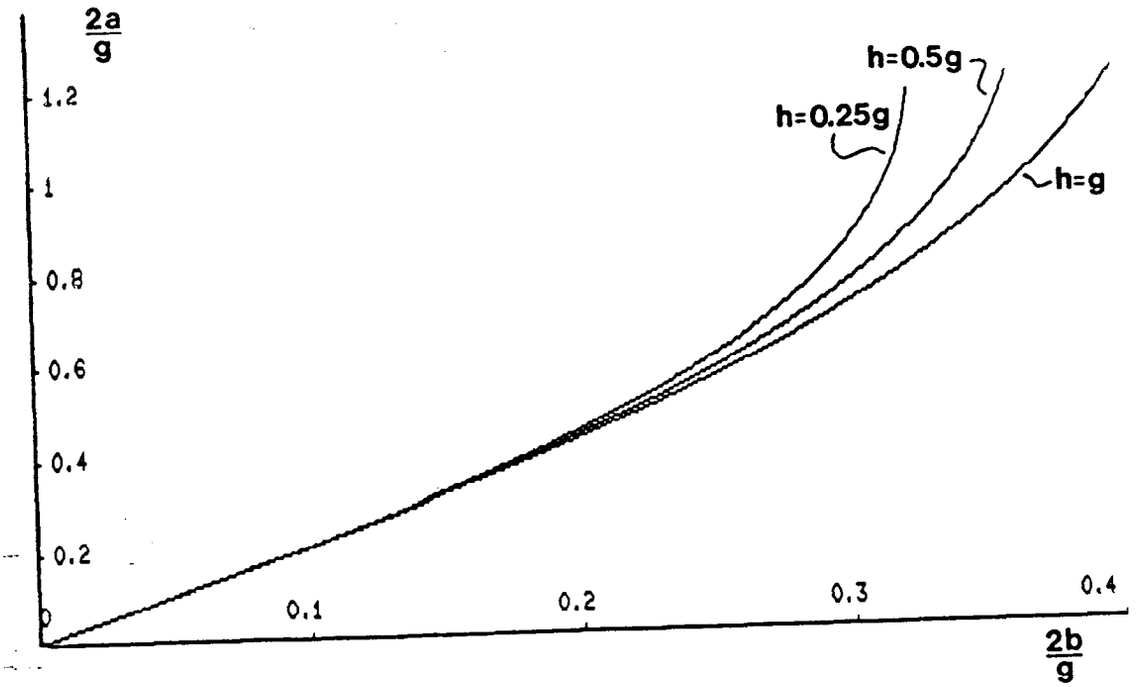

Fig. 4

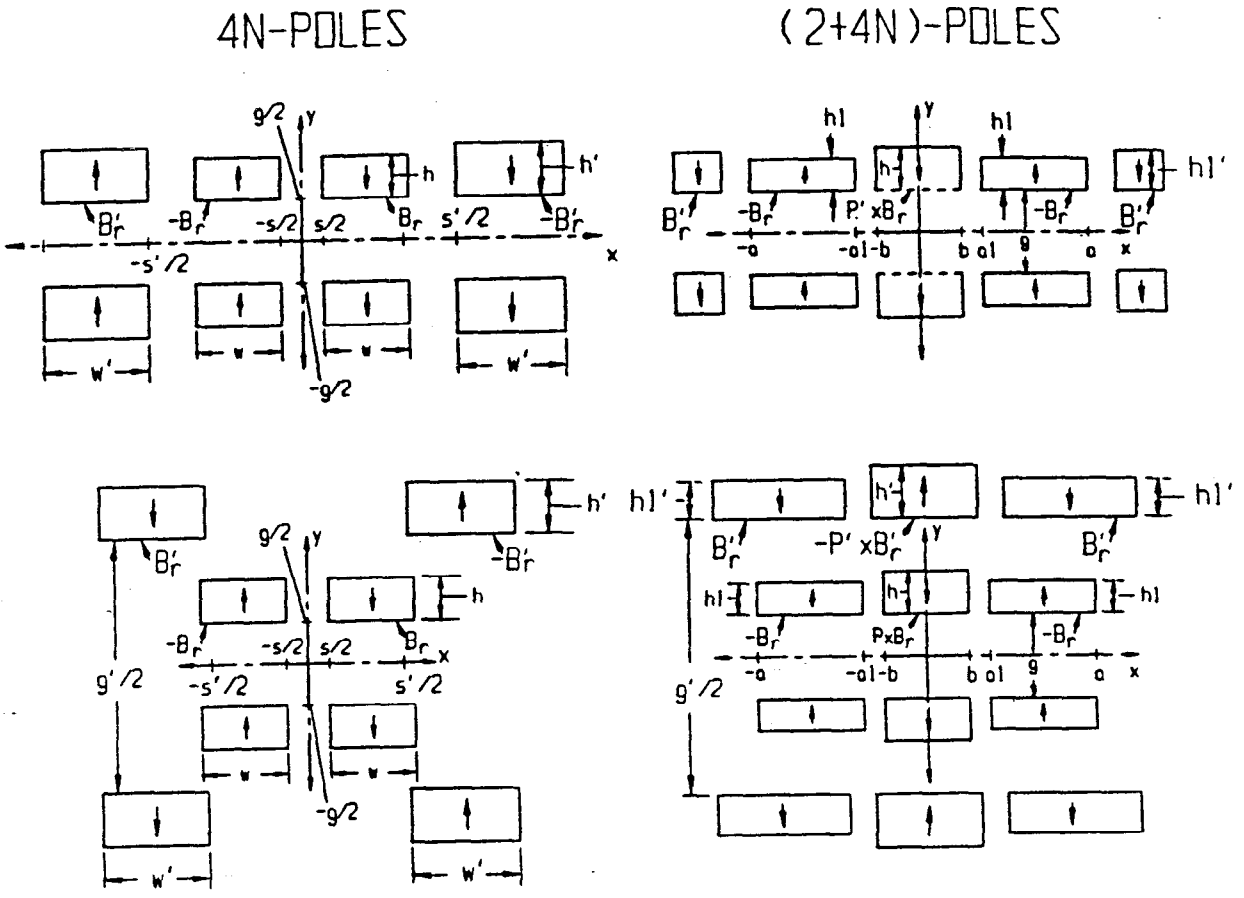
4N-POLES
(2+4N)-POLES
g/2
y
h
h'
B'_r
$-B_r$
-s/2
s/2
B_r
s'/2
$-B'_r$
x
-s'/2
w'
w
-g/2
hl
hl'
P'xB_r
-a
-a1
-b
b
a1
g
a
g'/2
$-P'xB'_r$
PxB_r

Fig. 5

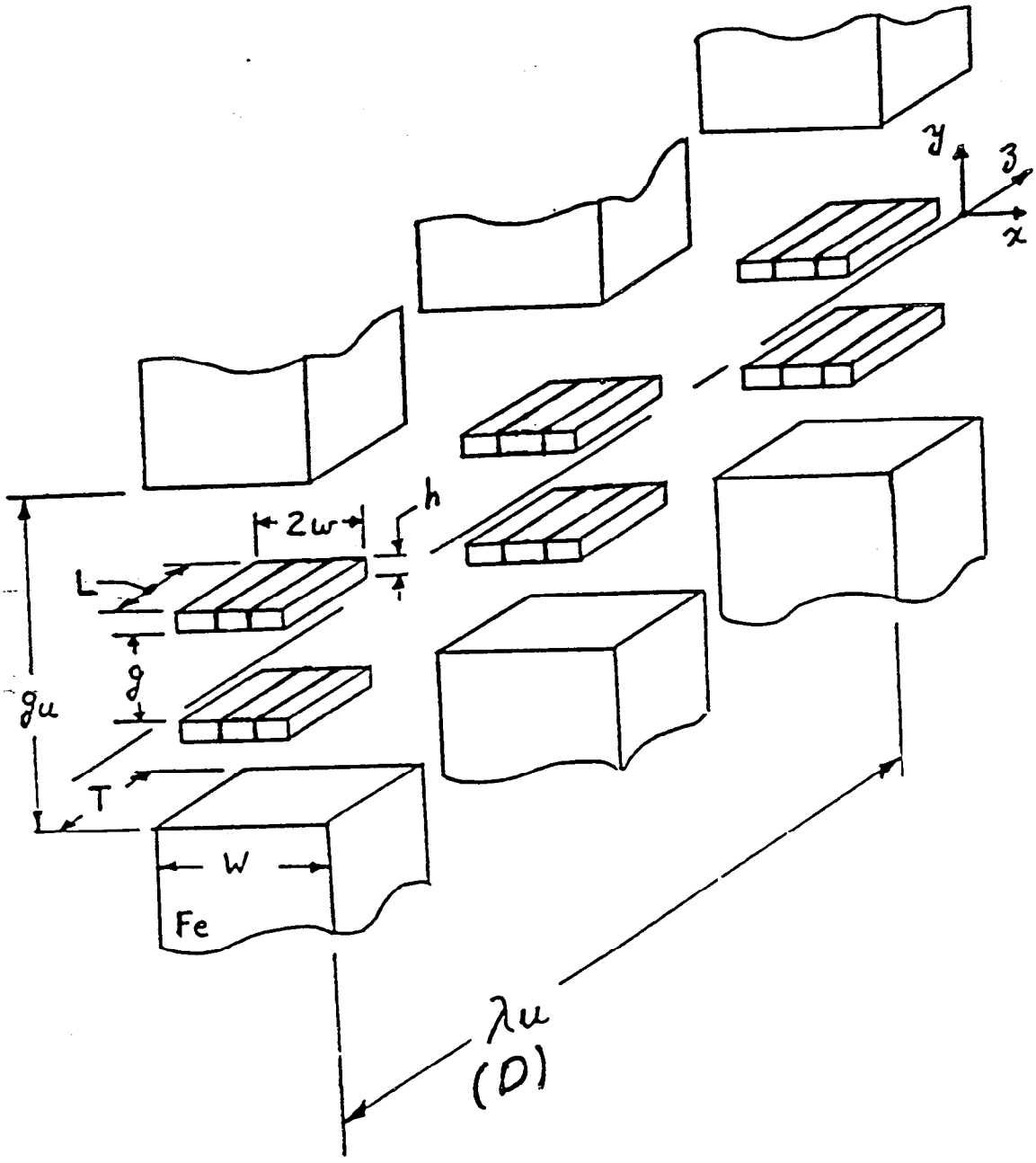

Fig. 6